

# Effects of Copper Doping on Microstructural Evolution in Eutectic SnBi Solder Stripes under Annealing and Current Stressing

CHIH-MING CHEN,<sup>1,3</sup> CHIH-CHIEH HUANG,<sup>1</sup> CHIEN-NENG LIAO,<sup>2</sup> and KUEN-MING LIOU<sup>2</sup>

1.—Department of Chemical Engineering, National Chung Hsing University, Taichung 402, Taiwan, R.O.C. 2.—Department of Materials Science and Engineering, National Tsing Hua University, Hsinchu 30013, Taiwan, R.O.C. 3.—e-mail: chenmc@dragon.nchu.edu.tw

Effects of Cu doping on the microstructural evolution in the eutectic SnBi solder stripes under annealing and current stressing were investigated. Coarsening of the Bi grains was observed in the eutectic SnBi solder upon annealing at 85°C. Doping of 1 wt.% Cu could significantly reduce the grain coarsening rate from 2.8 to 0.5  $\mu\text{m}^3/\text{h}$ . In addition to grain coarsening, mass accumulation of Bi at the anode and solder depletion at the cathode of the eutectic SnBi solder stripe stressed by a current of  $1.3 \times 10^4 \text{ A/cm}^2$  at 85°C were also observed. Doping of 1 wt.% Cu could also reduce the grain coarsening of the solder under current stressing; however, it resulted in an enhancement of the electromigration effect. Accumulation of Bi at the anode and the solder depletion at the cathode became more severe in the Cu-doped solder stripe.

**Key words:** Electromigration, grain coarsening, microstructure

## INTRODUCTION

Due to the detrimental impact of Pb toxicity on the environment and human health, searching for a proper Pb-free solder to replace the Pb-containing solder is an urgent issue in electronic packaging. With a lower melting point and coefficient of thermal expansion (CTE) in comparison with the eutectic SnPb alloy, the eutectic SnBi alloy (Sn-58 wt.% Bi) is a highly potential replacement, and is especially recommended to apply to the processes that are sensitive to temperature or thermal damage.<sup>1</sup> The eutectic SnBi solder has an undesired characteristic of the microstructural instability that can lead to a severe grain coarsening at elevated temperatures, resulting in a degradation of the mechanical properties. However, the severe grain coarsening can be significantly improved by doping small amounts of alloying element into the solder.

Miao et al.<sup>2</sup> found that the grain size in the solder doped with 1 wt.% Cu after a long-term annealing was quite uniform and much smaller compared to the eutectic SnBi solder. However, in their study, only microstructural examinations were conducted and no information on the kinetic analysis of the grain coarsening behavior was available.

Miniaturization is another important issue in electronic packaging. However, as the scale of the solder joint reduces to a level at which the average current density in the solder joint reaches  $10^3$  to  $10^4 \text{ A/cm}^2$ , electromigration may become a serious reliability concern. Electromigration refers to the phenomenon of atomic movement along the direction of electron flow.<sup>3</sup> Relevant studies indicate that electromigration can induce significant microstructural changes and different intermetallic growth in the solder joint systems.<sup>4–13</sup> The microstructural changes include void nucleation and propagation, hillock formation, and phase segregation. In the eutectic SnPb solder, it was found that

(Received October 31, 2006; accepted March 8, 2007; published online June 12, 2007)

electromigration could force Pb atoms to migrate along the direction of electron flow and accumulate at the anode side.<sup>6,8</sup> On the contrary, Sn atoms moved in the opposite direction and segregated at the cathode side. The eutectic SnBi solder also exhibited a similar electromigration behavior, i.e. mass accumulation of Bi was observed at the anode side and a Sn-rich region was formed at the cathode side.<sup>11,12</sup> Yang et al.<sup>11</sup> inferred that Bi atoms behaved like Pb in eutectic SnPb solder, which would migrate along the direction of electron flow toward the anode side and accumulate there.

The improvement of microstructural instability of the eutectic SnBi solder by doping Cu has been reported as mentioned above, but the relevant kinetic information is unavailable. The first aim of this study was to conduct the kinetic analysis of the grain coarsening behaviors in the eutectic SnBi solder without and with the doping of Cu. Comparisons of the microstructures and the kinetic analysis between these two solders under annealing was also made to have a detailed understanding of the effects of Cu doping. Electromigration behaviors of the eutectic SnBi solder have been reported previously,<sup>11,12</sup> but the solder doped with Cu is not studied yet. Since the Cu doping has a significant effect on the microstructural evolution in the eutectic SnBi solder, it may affect the Bi diffusion and lead to a different electromigration behavior. Therefore, the second aim of this present study was to investigate the effects of Cu doping on the electromigration behaviors of the eutectic SnBi solder.

## EXPERIMENTAL PROCEDURES

Figure 1a shows the schematic diagram of the specimen for both the annealing and electromigration tests. A bi-layer of Ta/Cu thin film was deposited on an oxidized Si wafer using electron beam evaporation. The thickness of Ta and Cu was 200 and 4,000 Å, respectively. By using photolithography and lift-off technique, a Ta/Cu stripe with square pads at the two ends was patterned. The dimension of the stripe was 10 mm in length and 300 μm in width. The Cu stripe was coated with flux. Then a tiny solder piece was placed on the center of the stripe. Two types of the solder alloys, the eutectic SnBi (Sn-58 wt.% Bi) and that doped with 1 wt.% Cu (Sn-57 wt.% Bi-1 wt.% Cu), were prepared. After reflow for 3 min, the solder piece transformed into a bump on the Cu stripe. The reflow temperatures for the Sn-58 wt.% Bi and Sn-57 wt.% Bi-1 wt.% Cu solders were 160°C and 200°C, respectively. The solder bump was polished down using ultra-fine sandpapers and 0.3 μm Al<sub>2</sub>O<sub>3</sub> suspension. After careful polishing, a solder stripe with approximately 20 μm thickness was fabricated on the Cu stripe. Figure 1b shows the plan-view scanning electron microscopy (SEM) image of eutectic SnBi solder stripe. The length of the solder stripe is around 1,000 μm. To reveal the

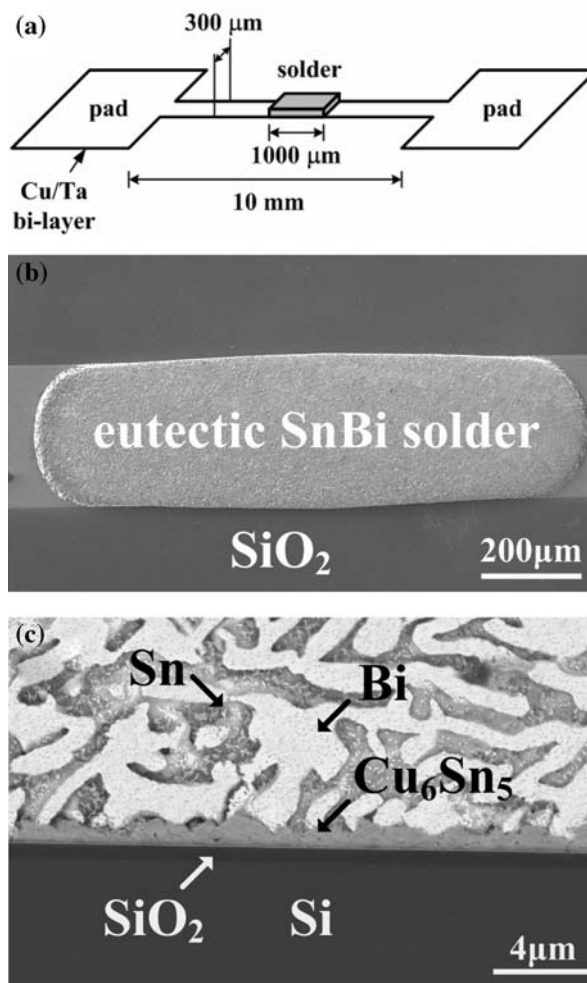


Fig. 1. (a) Schematic diagram of the specimens for annealing and electromigration tests. (b) Plan-view and (c) cross-sectional SEM images of the eutectic SnBi solder stripe.

microstructure of the solder/Cu contact interface, the solder stripe was cross-sectioned in a direction perpendicular to the stripe length using sandpapers and Al<sub>2</sub>O<sub>3</sub> suspensions. For a better observation of the cross section, the specimen was dipped into an etching solution of 2% HCl + 5% HNO<sub>3</sub> + 93% CH<sub>3</sub>OH for 10 sec to remove part of the Sn matrix. Figure 1c shows the cross-sectional SEM image of the solder/Cu interface, which reveals that the Cu layer underneath the solder is entirely reacted and transformed into the Cu<sub>6</sub>Sn<sub>5</sub> intermetallic layer. The thickness of the Cu<sub>6</sub>Sn<sub>5</sub> layer is about 1 μm. The solder stripe presents a two-phase microstructure where the bright Bi-rich phase is dispersed randomly in the continuous dark Sn-rich matrix.

To perform the annealing test, the specimens were put into a furnace set at 85°C for 24 to 240 h. For the electromigration test, a DC power supply was connected to the Cu stripe at its two end pads. A thermocouple was attached on the Cu stripe. By turning on the power supply, an electric current of

0.8 A passed through the Cu stripe. At the center of the Cu stripe, most of the electric current passed through the solder stripe due to its lower resistance compared to the thin  $\text{Cu}_6\text{Sn}_5$  and Ta layers. By comparing the resistance of these three parallel materials, the effective current density in the solder stripe was calculated to be  $1.3 \times 10^4 \text{ A/cm}^2$ . After the power supply was turned on, the Cu stripe was heated due to Joule heating. The thermocouple revealed that the temperature stayed around  $85 \pm 3 \text{ }^\circ\text{C}$  after 10 min of current stressing. The stressing time was set from 24 to 240 h. After annealing and current stressing, the solder stripes were slightly polished to remove the oxidant surface, so that a clear microstructure could be observed using SEM. Composition analysis was carried out using energy dispersive x-ray analyzer (EDX). Size measurements were performed using an image processing system.

## RESULTS AND DISCUSSION

### Effects of Cu Doping under Annealing

Figure 2 shows the enlarged plan-view SEM images of one end of the as-fabricated solder stripes, where (a) and (b) represent Sn-58 wt.%Bi and Sn-57 wt.%Bi-1 wt.%Cu, respectively. Since the microstructures were similar for the two ends of

the solder stripes, the microstructure of only one end was shown. In these two solders, the Bi grains were uniformly distributed in the Sn matrix. Finer grain microstructure was found in the Cu-doped solder. After annealing at  $85^\circ\text{C}$  for 240 h, the Bi grains in these two solders coarsened as shown in Fig. 3. In Fig. 3b, it was also found that many small  $\text{Cu}_6\text{Sn}_5$  particles precipitated inside the Cu-doped solder. These  $\text{Cu}_6\text{Sn}_5$  particles were marked by white circles for recognition since its color was quite similar to the Sn matrix. The grain coarsening of Bi in the Cu-doped solder was not as significant as that in the eutectic SnBi solder. This observation was similar to the results reported by Miao et al.,<sup>2</sup> which also found a finer microstructure of the Bi grains in the Cu-doped SnBi solder after solid-state annealing.

In a two-phase alloy, a high density of small grains tends to coarsen into a lower density of larger grains, so as to reduce the overall interfacial area as well as the interfacial free energy. Therefore, the total number of grains decreases and the average radius ( $\bar{r}$ ) of the grains increases upon increasing the annealing time. Generally, the grain coarsening obeys the following relationship:<sup>14</sup>

$$(\bar{r})^3 - (\bar{r}_0)^3 = kt \quad (1)$$

where  $\bar{r}_0$  is the average radius of the grain at annealing time  $t = 0$  and  $k$  is the coarsening rate

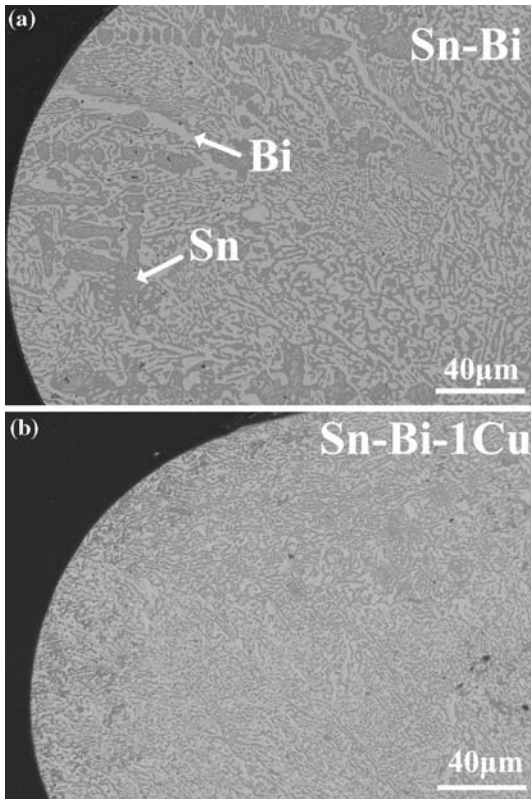


Fig. 2. Plan-view SEM images of one end of the as-fabricated Sn-58 wt.% Bi and Sn-57 wt.%Bi-1 wt.%Cu solder stripes.

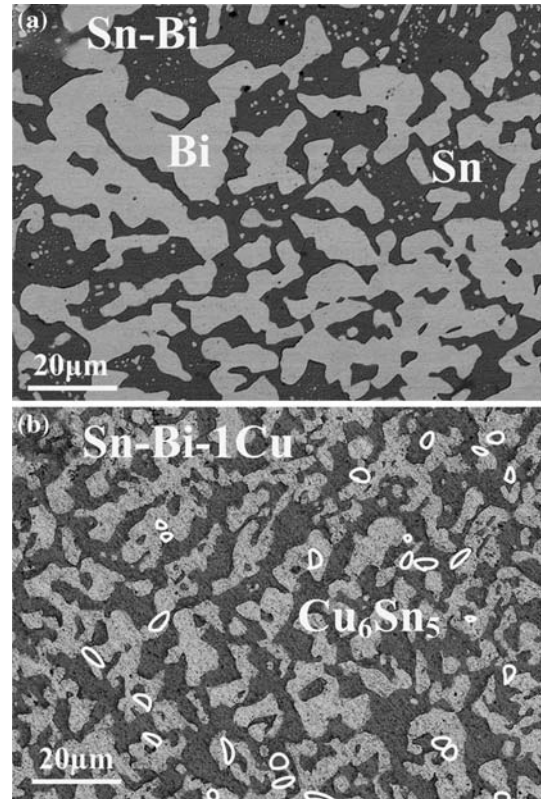


Fig. 3. SEM images of the (a) Sn-58 wt.%Bi and (b) Sn-57 wt.%Bi-1 wt.%Cu solder stripes after annealing at  $85 \text{ }^\circ\text{C}$  for 240 h.

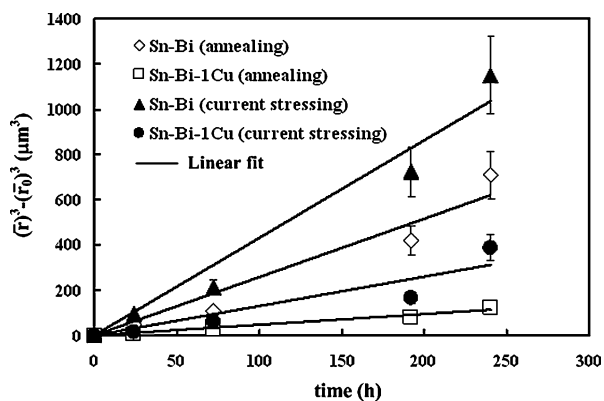


Fig. 4. Average radius of the Bi grains as a function of the annealing (stressing) time.

constant. The shape of the Bi grains was very non-uniform which made its radius difficult to measure. But for simplification, the Bi grains were taken as spheres. First, the overall cross-sectional area of the Bi grains on the stripe surface was measured. Then by dividing the overall area by the total grain number, the average cross-sectional area of the Bi grain was obtained. The average area was assumed to be equal to  $\pi\bar{r}^2$  and the average radius ( $\bar{r}$ ) was calculated. The average radii of the Bi grains after various annealing times were calculated and the results were shown by the hollow symbols in Fig. 4. To confirm the validity of Eq. 1, Fig. 4 was generated by taking  $(\bar{r})^3 - (\bar{r}_0)^3$  along the vertical axis and annealing time,  $t$ , along the transverse axis. The results of the linear fits indicated that the grain coarsening of Bi approximately followed Eq. 1. The slopes of the linear fit, i.e. the coarsening rate constants,  $k$ , were calculated and listed in Table I. The value of  $k$  was reduced from 2.8 to 0.5  $\mu\text{m}^3/\text{h}$  when the eutectic SnBi solder was doped with 1 wt.% Cu, which indicated that small amounts of Cu doping could significantly reduce the grain coarsening rate of Bi. As shown in Fig. 3b, the Cu that was doped into the solder reacted with Sn and many small  $\text{Cu}_6\text{Sn}_5$  particles were formed inside the solder. These particles might act as obstacles which retarded the movement of the grain boundary, thus leading to a reduced grain coarsening rate.

**Table I. Coarsening Rate Constants of the Bi Grains in the Eutectic SnBi Solder with and without the Doping of 1 wt.% Cu**

solder type (reaction condition)	coarsening rate constant ( $\mu\text{m}^3/\text{h}$ )
Sn-Bi (annealing)	2.8
Sn-Bi-1Cu (annealing)	0.5
Sn-Bi (current stressing)	4.6
Sn-Bi-1Cu (current stressing)	1.4

### Effects of Cu Doping under Current Stressing

Figure 5 shows the enlarged plan-view SEM images of the two ends of the solder stripes after current stressing for 240 h, where the upper- and lower-half images represent Sn-58 wt.%Bi and Sn-57 wt.%Bi-1 wt.%Cu, respectively. Compared to Fig. 2, grain coarsening was observed in the two current-stressed solder stripes. The radii of the Bi grains in the current-stressed solder stripes for various stressing times were estimated and shown in Fig. 4. The results of the linear fits revealed that the grain coarsening of Bi under current stressing also approximately obeyed Eq. 1. According to the linear fit, the coarsening rate constants were calculated and listed in Table I. Compared to the annealing data, the coarsening rate constants in these two solders under current stressing were larger. However, if these two current-stressed solders were compared with each other, the grain coarsening rate in the Cu-doped solder was smaller than that in the eutectic SnBi solder, which was the same as the annealing case.

The enhanced grain coarsening in the SnBi solder by current stressing was reported previously<sup>12</sup> and was also observed in the eutectic SnPb solder.<sup>13</sup> However, the mechanism was still unknown. In addition to the grain coarsening, the current stressing had another significant effect on the microstructural evolution of the SnBi solder. As shown in Fig. 5, a thick continuous layer of Bi accumulation at the anode end and a solder depleted region (as marked by a dotted line) at the cathode end in these two solder stripes were observed. This observation was similar to the previous studies.<sup>11,12</sup> Electromigration could induce the atomic migration of Bi along with the electron flow and moved toward the anode side, which resulted in the mass accumulation of Bi at the anode. Enlarged SEM images of the solder depleted regions were shown in Fig. 6. It was found that not only Bi but also Sn were removed by electromigration since a solder region near the cathode end disappeared and the underneath  $\text{Cu}_6\text{Sn}_5$  intermetallics and Ta layer were exposed. It was also found that the solder depletion (the region of Ta +  $\text{Cu}_6\text{Sn}_5$ ) was more significant in the Cu-doped solder than in the eutectic SnBi solder. For other stressing times from 24 to 192 h, a similar Bi accumulation at the anode end was also observed. Figure 7 depicts the thickness of the Bi accumulation layer as a function of stressing time. Each thickness in Fig. 7 was an average value, which was obtained by dividing the layer's total area by the arc length of the anode edge. As shown in Fig. 7, the Bi accumulation layer in the Cu-doped solder was thicker than that in the eutectic SnBi solder.

According to the above results, doping of small amounts of Cu into the eutectic SnBi solder could significantly reduce the grain coarsening rate when the solder is under current stressing. A slower grain

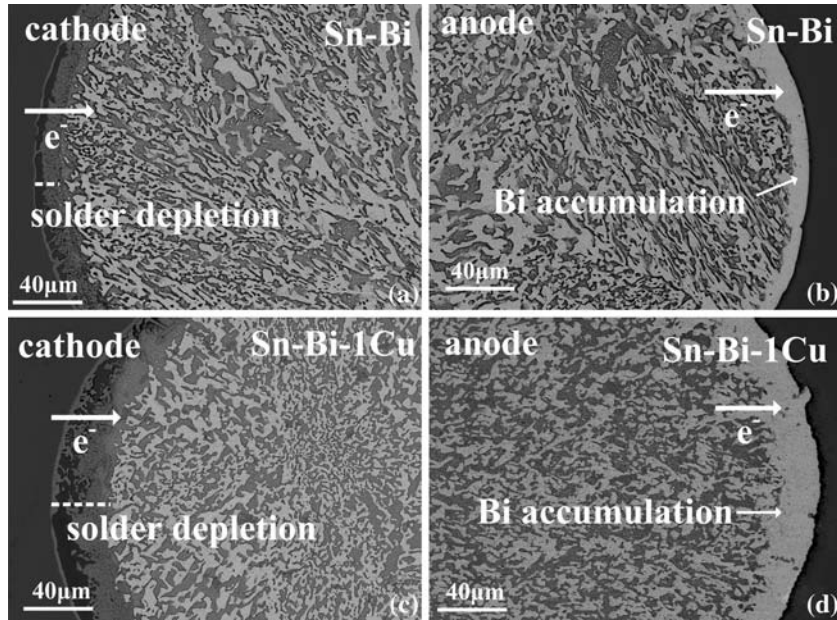


Fig. 5. Plan-view SEM images of the two ends of the Sn-58 wt.%Bi and Sn-57 wt.%Bi-1 wt.%Cu solder stripes after current stressing for 240 h.

coarsening rate could lead to an approximately consistent and uniform microstructure in the solder, which might reduce the degradation of the mechanical properties. However, the above results

also indicated that the electromigration effect might be enhanced significantly by doping Cu into the solder. As shown in Fig. 7, the thickness of the Bi accumulated layer in the Cu-doped solder was larger than that in the eutectic SnBi solder. For a real solder joint using the eutectic SnBi solder, doping small amounts of Cu is a useful method to reduce the non-uniform grain coarsening in the bulk solder when the solder joint undergoes only solid-state annealing. However, once the solder joint is current-stressed, electromigration will result in a larger amount of the Bi accumulation at the anode-end joint interface, which may cause some negative impacts on the joint reliability. The mechanical strength of the joint interface will significantly degrade due to the formation of a brittle Bi layer at

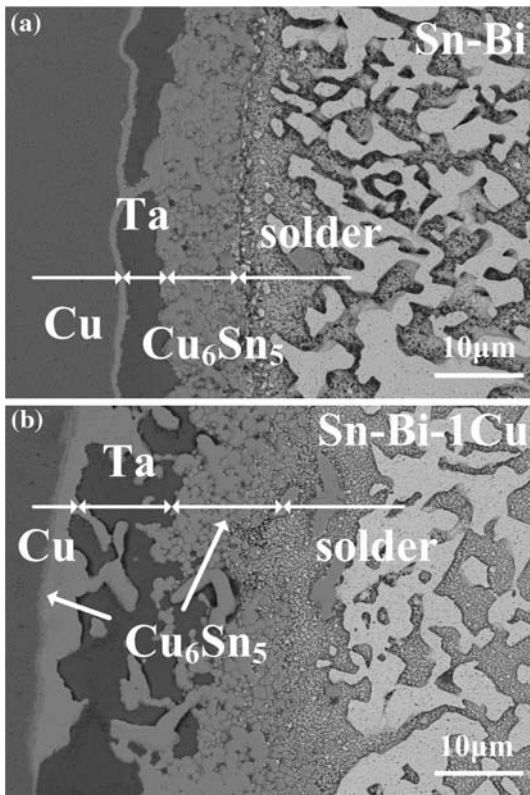


Fig. 6. Enlarged SEM images of the cathode ends of the Sn-58 wt.%Bi and Sn-57 wt.%Bi-1 wt.%Cu solder stripes after current stressing for 240 h.

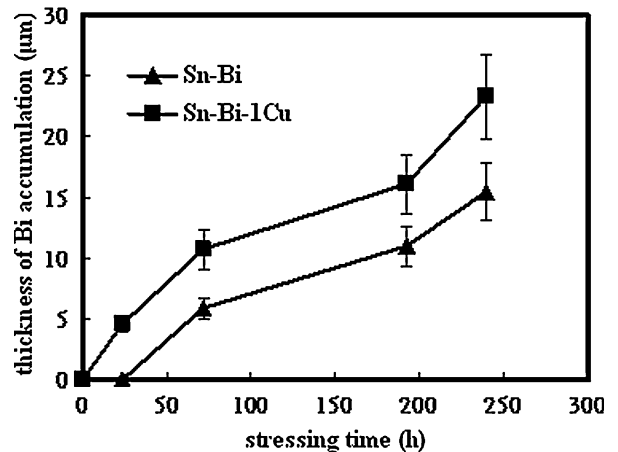


Fig. 7. Thickness of the Bi accumulated layer at the anode end of the solder stripe as a function of the stressing time.

the interface. In addition, Joule heating will become more serious at the joint interface due to the higher resistivity of Bi. Another negative influence was shown in Fig. 6. More solder was removed away from the cathode end of the Cu-doped solder stripe, which might lead to more severe void formation.

In a eutectic microstructure, the Bi atoms can diffuse through the Sn-rich phase, the Bi-rich phase, and the Sn/Bi grain boundaries. In general, the grain boundary acts as a fast diffusion path due to its more open structure, and therefore should play an important role in the Bi diffusion. As shown in Table I, the grain coarsening rate was significantly reduced from 4.6 to 1.4  $\mu\text{m}^3/\text{h}$  when 1 wt.%Cu was doped into the eutectic SnBi solder. With a finer grain size in the initial condition and a slower grain coarsening rate under current stressing, the Cu-doped solder exhibited a finer microstructure which could offer a higher density of the grain boundary for more Bi diffusion toward the anode. Therefore, more accumulation of Bi at the anode end of the Cu-doped solder stripe was observed.

### CONCLUSION

Microstructural instability of the eutectic SnBi solder caused an extensive and non-uniform grain coarsening when the solder was annealed at elevated temperatures. Doping 1 wt.%Cu into the solder could significantly reduce the grain coarsening rate and lead to a finer and uniform microstructure. The reduced effect was ascribed to the formation of many small  $\text{Cu}_6\text{Sn}_5$  particles inside the solder, which acted as obstacles to retard the movement of the grain boundary. However, the electromigration effect of the eutectic SnBi solder was enhanced by the doping of Cu. Stressed by a current density of  $1.3 \times 10^4 \text{ A/cm}^2$  at 85°C, a large number of Bi accumulated at the anode end and a solder depleted

region was formed at the cathode end of the solder stripes with and without the doping of Cu. However, more Bi accumulation and more severe solder depletion were observed in the Cu-doped solder stripe. The enhanced electromigration effect should be related to the reduced grain coarsening in the Cu-doped solder, which provided a higher density of the grain boundary for more Bi migration toward the anode end.

### ACKNOWLEDGEMENT

The authors wish to acknowledge the financial support of National Science Council of Taiwan, ROC through Grant NSC 94-2214-E-005-008.

### REFERENCES

1. F. Hua, Z. Mei, and J. Glazer, *Proc. 48th Electronic Components and Technology Conf.* 277 (1998).
2. H.W. Miao and J.G. Duh, *Mater. Chem. Phys.* 71, 255 (2001).
3. H.B. Huntington, in: A.S. Nowick, J.J. Burton (Eds.), *Diffusion in Solids: Recent Developments*, Academic Press, New York, 303–352 (1975).
4. E.C.C. Yeh, W.J. Choi, K.N. Tu, P. Elenius, and H. Balkan, *Appl. Phys. Lett.* 80, 580 (2002).
5. Y.C. Hu, Y.H. Lin, C.R. Kao, and K.N. Tu, *J. Mater. Res.* 18, 2544 (2003).
6. S. Brandenburg and S. Yeh, *Proc. Surface Mount Int. Conf. and Exposition*, San Jose, CA 337 (1998).
7. J.Y. Choi, S.S. Lee, and Y.C. Joo, *Jpn. J. Appl. Phys.* 41, 7487 (2002).
8. G.A. Rinne, *Microelectron. Reliab.* 43, 1975 (2003).
9. C.M. Chen and S.W. Chen, *J. Appl. Phys.* 90, 1208 (2001).
10. C.Y. Liu, C. Chen, and K.N. Tu, *J. Appl. Phys.* 88, 5703 (2000).
11. Q.L. Yang and J.K. Shang, *J. Electron. Mater.* 34, 1363 (2005).
12. L.T. Chen and C.M. Chen, *J. Mater. Res.* 21, 962 (2006).
13. H. Ye, C. Basaran, and D.C. Hopkins, *Int. J. Solids Struct.* 41, 2743 (2004).
14. D.A. Porter and K.E. Easterling, *Phase Transformations in Metals and Alloys* (London, UK: Chapman & Hall, 1992), p. 315.